



Research Article

Heat transfer enhancement for corrugated facing step channels using aluminium nitride nanofluid - numerical investigation

Kafel AZEEZ¹, Abd Rahim ABU TALIB², Riyadh IBRAHEEM AHMED^{3,*}

¹Renewable Energy Research Centre, University of Anbar, 44016, Anbar, Iraq

²Aerodynamics, Heat Transfer & Propulsion Group, Department of Aerospace Engineering, University Putra Malaysia, 43400 Serdang, Selangor, Malaysia

³Ministry of High Education and Scientific Research and Science and Technology, 100011, Baghdad, Iraq

ARTICLE INFO

Article history

Received: 17 January 2021

Accepted: 04 April 2021

Keywords:

CFD; Heat Transfer; Heat Exchanger; Nanofluid; Numerical Analysis

ABSTRACT

The present work carries out a three-dimensional numerical analysis study of Aluminium Nitride (AlN)-water hybrid nanofluid enhanced heat transfer in laminar forced convection flow heat exchanger with four different channels, flat, backward facing step, triangle and trapezoidal facing step channels. The influence of different Reynolds number ($100 \leq Re \leq 1500$) and different solid nanoparticles volume fraction (1% and 4%) on the heat transfer and fluid flow were numerically investigated. The numerical analysis was carried out by using a laminar model of ANSYS-Fluent CFD code and the governing equations were resolved using the finite volume method. The results indicate that the thermal conductivity of the nanofluids increases with the increase values of both the nanoparticles volume fractions and Reynolds number, compared with base fluids. Likewise, the pressure drop showed slightly increased due to the increased of both parameters. The use of high nanoparticles volume fractions (4% volume) nanofluid corresponded with the use of four different channel designs resulted in heat transfer augmentation about 30% when compared to that pure water for the trapezoidal channel.

Cite this article as: Azeez K, Abu Talib AR, Ibraheem Ahmed R. Heat transfer enhancement for corrugated facing step channels using aluminium nitride nanofluid - numerical investigation. J Ther Eng 2022;8(6):734–747.

INTRODUCTION

Nowadays, the most encouraging process to enhance heat transfer with suitable pressure drop of heat exchanger is the use of hybrid solid nanoparticles disseminated in pure water as a working fluid. Nanofluid, heat transfer

and pressure drop enhancement studies of heat exchanger have been interested for flow region through backward facing step corrugated channel. The application of nanofluids is believed to have a strong potential for enhancing

*Corresponding author.

*E-mail address: engriyadh64@gmail.com

This paper was recommended for publication in revised form by Regional Editor Mustafa Kılıç



the characteristics of heat transfer of heat exchangers, for example [1-3]. Due to many engineering implementation such as electronic cooling devices, combustors, flow around buildings, collectors, aerofoils and heat exchangers, there are quite a lot of studies in the literature focused on backward facing step flow. Geridönmez and Öztop [4] performed a numerical study to investigate the effect of mixed convection flow of a hybrid nanofluid in a backward facing step channel in the presence of a uniform partial magnetic field. The founding disclose that the smallest convective heat transfer is achieved in the step-centred partial magnetic field and the increase in magnetite nanoparticles has a significant influence on convective heat transfer. Abu-Mulaweh [5] conducted an experimental study on laminar flow mixed convection over horizontal, vertical and inclined, forward and backward facing steps channel. It was found that the introduction of backward- and forward-facing steps increases the turbulence intensity of the velocity and temperature fluctuations downstream of the step. The results also reveal that the maximum local Nusselt number is approximately twice for the case of the backward-facing step and three times for the case of the forward-facing step than that of the flat plate value at similar flow and thermal conditions. Barkley et al. [6] studied the longitudinal stability of Reynolds numbers between 450 -1050 for backward-facing step flow.

Moreover, the velocity distribution and the reattachment length on three-dimensional flow downstream of a backward facing step were conducted by Armaly et al. [7] utilizing Laser-Doppler Velocimeter (LDV). The results explore the variation of separation length with diverse flow and Reynolds number that were characterized by the difference of the separation length. Sherry et al. [8] performed an experimental work on the recirculation region created downstream of a forward facing step sinking in a turbulent boundary layer. Herein, the mechanisms affecting the turbulent mixing within the boundary layer, the velocity deficit in the boundary layer and the technique disturbing the re-attachment area were defined and deliberated.

To procure better thermal properties in heat transfer implementation, Nano-sized particles (≤ 100 nm) are introduced in the base fluid such as Glycol Ethylene or pure water. What does the Nanofluid do to the fluid? It improves heat transfer characteristics with slight pressure drop. Sivakumar et al [9] investigated the use of various metal oxide nanofluids Al_2O_3 +water, CuO+water, and CuO+EG in U-shaped serpentine microchannel heat sink. The founding showed that the thermal conductivity of nanofluids was increased for all concentrations (from 0.01 to 0.3% volume), compared with base fluids. Within the same field of investigations, Mohammed et al. [10] carried out an experimental and numerical examination to test the heat transfer and friction factor of Al_2O_3 /Ethylene glycol-water nanofluid passing through a straight channel. The results reveal that the heat transfer coefficient and the

friction factor increases with an increase of the nanoparticles concentration at the same Re .

Abu-Nada [11] conducted a numerical investigation on the heat transfer advantage through backward facing step utilizing various types of nanofluid. Abu-Nada found out that the better heat transfer characteristic obtained by low nanoparticles thermal conductivity and averaged heat transfer improved as nanoparticles volume fraction increase. Similarly, Kherbeet et al. [12] have conducted a numerical study on micro-scale backward facing step investigating three-dimensional Laminar mixed convection. The working fluid was EG-SiO₂ nanofluid with 0.04 volume fraction and nanoparticle diameters of 25 nm, the impact of step length was examined. Bayareh and Nourbakhsh [13] conducted a numerical simulation and analysis of heat transfer for different geometries of corrugated tubes in a double pipe heat exchanger. Results show that the maximum heat transfer corresponds to the convex-concave case in comparison with the smooth-smooth one. Heat transfer rate increases with the Reynolds number, but the slope of the increase for nanofluid is lesser than that for the pure fluid. Al-Aswadi et al. [14] studied the laminar flow over a backward facing step with various kinds of nanofluids of different concentration. They indicated that the highest velocity obtained by the nanofluid with SiO₂ nanoparticles, while the lowest velocity obtained with Au nanoparticles. On the same line, Kaouther et al. [15] conducted a three-dimensional computational analysis of hybrid nanofluid enhanced heat transfer in cross flow micro heat exchanger. The result proven that a suitable flow velocity and nanoparticles volume fraction can minimize the size of the heat exchanger. Likewise, the addition of nanoparticles has important result merely with high velocities ($u \geq 50$ mm/s). Equally important, Kilic and Ali [16] studied the effects of different volume ratio, different heat flux and different types of nanofluids (CuO-water, Al_2O_3 -water, Cu-water, TiO-water, and pure water) on heat transfer and fluid-flow. The results showed that by increasing volume ratio ($\phi = 2\%$ to 8%) the average Nusselt number may increase by 10.4%. it was also proven the using nanofluids (Cu-water) has an advantage over CuO-water, TiO-water, Al_2O_3 -water and purified water on the enhancement of the average Nusselt number (Nu). Plant and Saghir [17] examined the effect of high concentration aqueous alumina nanofluid on the heat transfer for different kind of heat sink equipped with porous media. The use of high concentration 2% volume alumina nanofluid together with the two channels resulted in a maximum enhancement of 24.5%.

The objective of this paper is to provide a fundamental analysis for the estimation of heat transfer enhancement and the effect of pressure drop through backward corrugated facing step channel with nanofluid. Numerically investigate the consequence effect of Reynolds number (100-1500) and the use of solid volume fraction nanoparticle AlN (1%-4%) on the fluid flow and heat transfer.

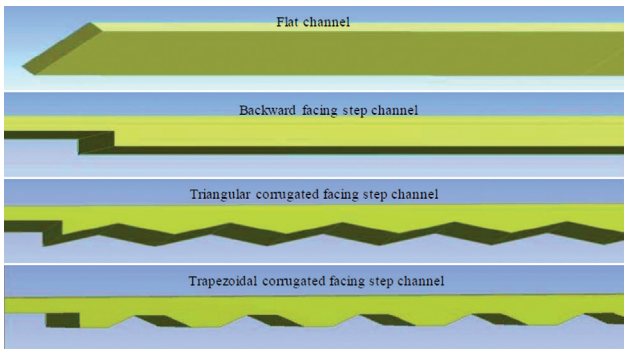


Figure 1. Schematic diagram of the domains of the flat, backward, triangular and trapezoidal facing-step channels with wavelength of 2 cm and amplitude height of 4 mm.

NUMERICAL MODEL

The geometrical models of the four types of channels used in this present study are depicted in Figure.1. The two models of interest were equipped with lower triangular and trapezoidal corrugated plates of wavelength (L_w) and amplitude height (a).

Mathematical Model

Following our previous investigations as in [18], the flow is considered incompressible, laminar, steady, and three-dimensional, while the nanofluid is set as Newtonian fluid. In addition, the blend of solid nanoparticles and water mixture entering the channels are presumed at the same temperature and at equal velocity. The numerical simulation has been conducted using predominated software (ANSYS-Fluent, 14.5). The nondimensional governing equations and vorticity transport are defined by the conservative equations indicated below:

Continuity equation:

$$\nabla \cdot (\rho_{nf} \vec{V}) = 0 \quad (1)$$

Momentum equation:

$$\nabla \cdot (\vec{V} \vec{V}) = -\frac{1}{\rho_{nf}} \nabla p_{nf} + \nu_{nf} \nabla^2 \vec{V} \quad (2)$$

Energy equation:

$$\nabla \cdot (\vec{V} T) = -\frac{1}{\rho_{nf} C_{p,nf}} k_{nf} \nabla^2 T \quad (3)$$

where, p_{nf} , ν_{nf} , $C_{p,nf}$ and k_{nf} are respectively the nanofluid pressure, dynamic viscosity, specific heat capacity and thermal conductivity

Thermophysical Properties of Nanofluids

The nanofluid thermophysical properties and the effective thermal conductivity could be calculated using the equations reflected by Ghasemi *et al.* [19] as:

$$k_{eff} = k_{static} + k_{Brownian} \quad (4)$$

where

$$k_{static} = k_{bf} \left[\frac{(k_{np} + 2k_{bf}) - 2\phi(k_{bf} + 2k_{np})}{(k_{np} + 2k_{bf}) - \phi(k_{bf} + 2k_{np})} \right] \quad (5)$$

k_{bf} and k_{np} are the thermal conductivity of the base fluid and the nanoparticle respectively.

The Brownian motion thermal conductivity is defined by the equation below and according to Vajjha and Das [20]

$$k_{Brownian} = 5 \times 10^4 \phi \beta \rho_{bf} C_{p,bf} \sqrt{\frac{KT}{2\rho_{np} R_{np}}} f(T, \phi) \quad (6)$$

where K is Boltzmann constant ($=1.38066 \times 10^{-23}$ J/K), β is a function of the liquid volume that exits with a particle material, $f(T, \phi)$ is a function of particle volume fraction and temperature.

The ratio between the effective dynamic viscosity of Nano and base fluids is calculated using the equation considered by Corcione [21]

$$\frac{\mu_{eff}}{\mu_{bf}} = \frac{1}{1 - 34.8 \left(\frac{d_{np}}{d_{bf}} \right)^{-0.3} \phi^{1.03}} \quad (7)$$

where μ_{eff} and μ_{bf} are the nanofluid and base fluid effective dynamic viscosity, d_{np} is the diameter of nanoparticle, d_{bf} is the equivalent diameter of base fluid $d_{bf} = [6M/N\pi\rho_{bf}]^{1/2}$, M is the base fluid molecular weight and ϕ is the nanoparticle volume fraction.

The effective nanofluid density can be defined in according to the equation specified by Corcione [21];

$$\rho_{eff} = (1 - \phi) \rho_{bf} + \rho_{np} \quad (8)$$

where ρ_{bf} is the base fluid density and ρ_{np} is the nanoparticle density.

Similarly, the nanofluid effective specific heat (C_p)_{eff} is computed for constant pressure by;

$$(c_p)_{eff} = \frac{(1 - \phi)(\rho c_p)_{bf} + \phi(\rho c_p)}{(1 - \phi)\rho_{bf} + \phi\rho_{np}} \quad (9)$$

where Cp_{nf} is the solid particles heat capacity and Cp_{bf} is the base fluid heat capacity.

The thermophysical properties of the AlN nanoparticles and distilled water based fluids at $T = 300$ K are given in Table 1.

The dimensionless parameters of Nu , Re and the friction factor calculated according to Eiamsa-Ard and Promvonge [22]:

Nusselt number

$$Nu = \frac{hD_h}{k} \tag{10}$$

Reynolds number

$$Re = \frac{\rho u_m D_h}{\mu} \tag{11}$$

where u_m is the mean velocity of the fluid. The hydraulic diameter is equal to $(D_h) = 4A/P$. where A is cross-section area and P is wetted perimeter.

The fully developed flow friction factor for is defined as:

$$f = \frac{2\Delta p D_h}{L \rho u_m^2} \tag{12}$$

Table 1. Thermophysical properties of the AlN nanoparticles and pure water at $T = 300$ K [21]

Properties	AlN nanoparticles	Water
(kg/m ³)	4175	996.5
Cp (J/kg·K)	692	4181
k (W/m·K)	8.4	0.613
μ (Ns/m ²)	–	1×10^{-3}
β (1/K)	5.5×10^{-6}	2.75×10^{-4}

To calculate the required parameters all the above equations have to be use accordingly using the values of the other perimeters within these equations as mentioned in following Table 2.

CFD Analysis

The geometrical dimensions of the heat exchangers models used in this study are illustrated in Figure 2. The total length of the channels is 110cm and with a height of 1 cm, adds to it the step height of the backward and corrugated plates, which is 0.5 cm. The combined length

Table 2. Effect of the nanoparticle volume fraction on other parameters

φ %	$f(T,\varphi)$	μ eff	k static	K Brow.	k eff	ρ eff	Cp eff
1	0.000320	0.00111	6.073E-01	1.248E-02	0.6197	1010.022	4107.4
2	0.000318	0.00118	6.128E-01	8.701E-03	0.6215	1022.244	4033.7
3	0.000316	0.00125	6.185E-01	7.447E-03	0.6259	1034.466	3961.7
4	0.000314	0.00133	6.241E-01	6.488E-03	0.6306	1046.688	3891.3

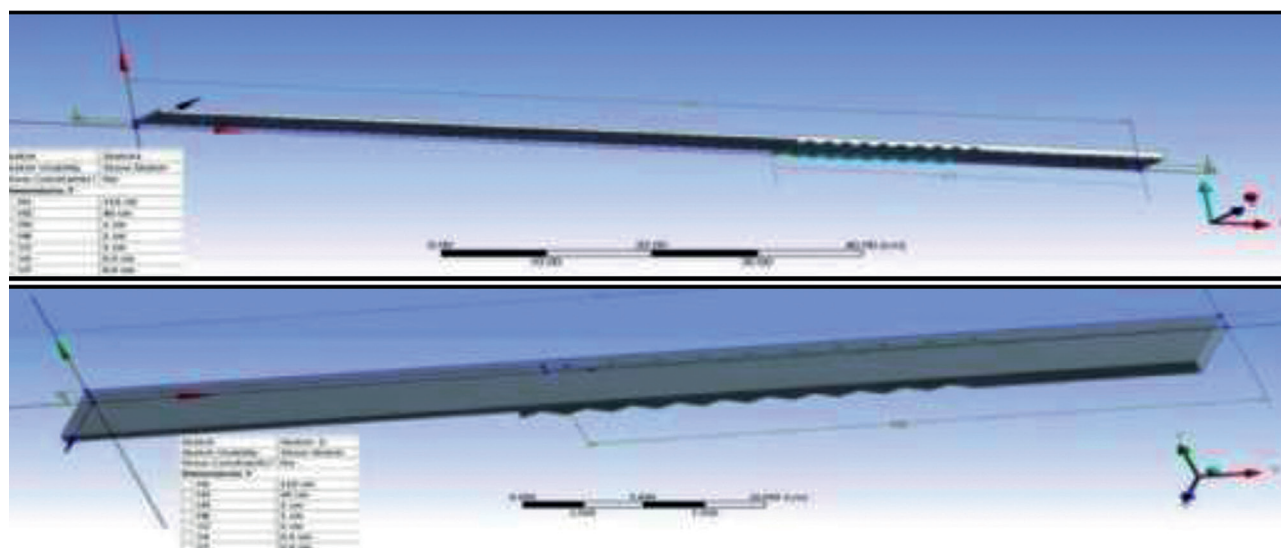


Figure 2. Geometrical shape and dimensions of triangular and trapezoidal facing-step channels models.

Table 3. Dimensions of the flat, back ward, triangle and trapezoidal-corrugated facing step channels

Facing Step Channel	Inlet Section (cm)	Corrugated Section (cm)	Outlet section (cm)	Height of Step (cm)
Flat	----	----	----	----
Back Ward	70	-----	40	0.5
Triangle Corrugated	70	20	20	0.5
Trapezoidal-Corrugated	70	20	20	0.5

Table 4. The influence of the grid intensity on the computational results

Grid number	Average Nusselt number	Relative error	Relative error
46875	6.1315	----	----
375000	7.8469	0.2186	21.86 %
1736110	8.9789	0.1261	12.61 %
3000000	9.6996	0.0743	7.43 %
5859375	9.7583	0.006015	0.6015 %

of the lower corrugated plate is 20 cm in length. In line with our previous investigation [18], the inlet section is considered a smooth adiabatic section and of 70cm in length, in order to create suitable boundary conditions. The outlet section is also considered a smooth adiabatic section but of 20cm in length. Table 3 depicts the dimensions of the flat, back ward, triangle and trapezoidal-corrugated facing step channels. Moreover, for the current study, the tests will be carried out for the triangular and trapezoidal with amplitude height ($a= 0.0, 0.1, 0.2, 0.3$ and 0.4 cm) and the wavelength ($L_w = 2, 4, 5$ and 10 cm). The nanoparticle size was set equal to 100 nm and the volume fractions from 1% to 4% were considered. The inlet temperature of the single flow nanofluid was 25°C and the constant wall heat flux was 24000 W/m². The test section wall is to be heated isothermally.

For the three-dimensional simulations, mesh was decided to be a symmetric grid to allow a larger mesh and reducing the running time. The grid is bunched in the locale of the inlet and over the corrugated surface to accurately capture the flow behaviour over these surfaces. The mesh structure was organized according to the flow conditions, with the aim of more accurate numerical results. The mesh numbers were intensified in some regions at the surface of lower plate for all channels

The finite volume method was considered to discretize the governing equations with suitable boundary conditions. In here, the Reynolds Average Navier Stokes equation is disbanded to generate the mesh. Simple explicit method, based on the time marching technique used to solve the energy and the vorticity transport equations.

Contrariwise, the stream function equation adapted the relaxation method for solution as defined by Anderson [23]. As the process to solve the governorate equation start iterating the solution, the stream function is counted and the vorticity transport and energy equations are disbanded to define the temperature and vorticity for the all nodes of the computational mesh of the domain. The iteration was persistent until the residual for most computational domain parameters reached the value less than 10^{-5} , for a time step of 10^{-3} .

Figure 3 depicts the CFD simulation velocity contour for four different configurations such as flat channel, back ward, triangular and trapezoidal facing step channels at constant Re of 250 with variation of the wavelength for 2, 4, 5 and 10 cm. It is clearly indicated that the enhancement in the heat transfer occurs at 2 cm wavelength for both the trapezoidal and triangular shapes in comparison to other geometrical configurations.

Grid Independence Test

To check the influence of the grid intensity on the computational results, five different sizes of grid generation were examined as illustrated in Table 4. Here, Figure 4 (a) and (b) illustrated the surface Nusselt number and pressure distribution along the bottom wall of trapezoidal corrugated facing step channel at $Re = 100$ (laminar flow region), $a = 4.0$ mm, $L_w = 20$ mm, have been investigated over these grid sizes. The results display that the grid size of 3000000 ensures the grid-independent test and it is therefore engaged throughout this Study.

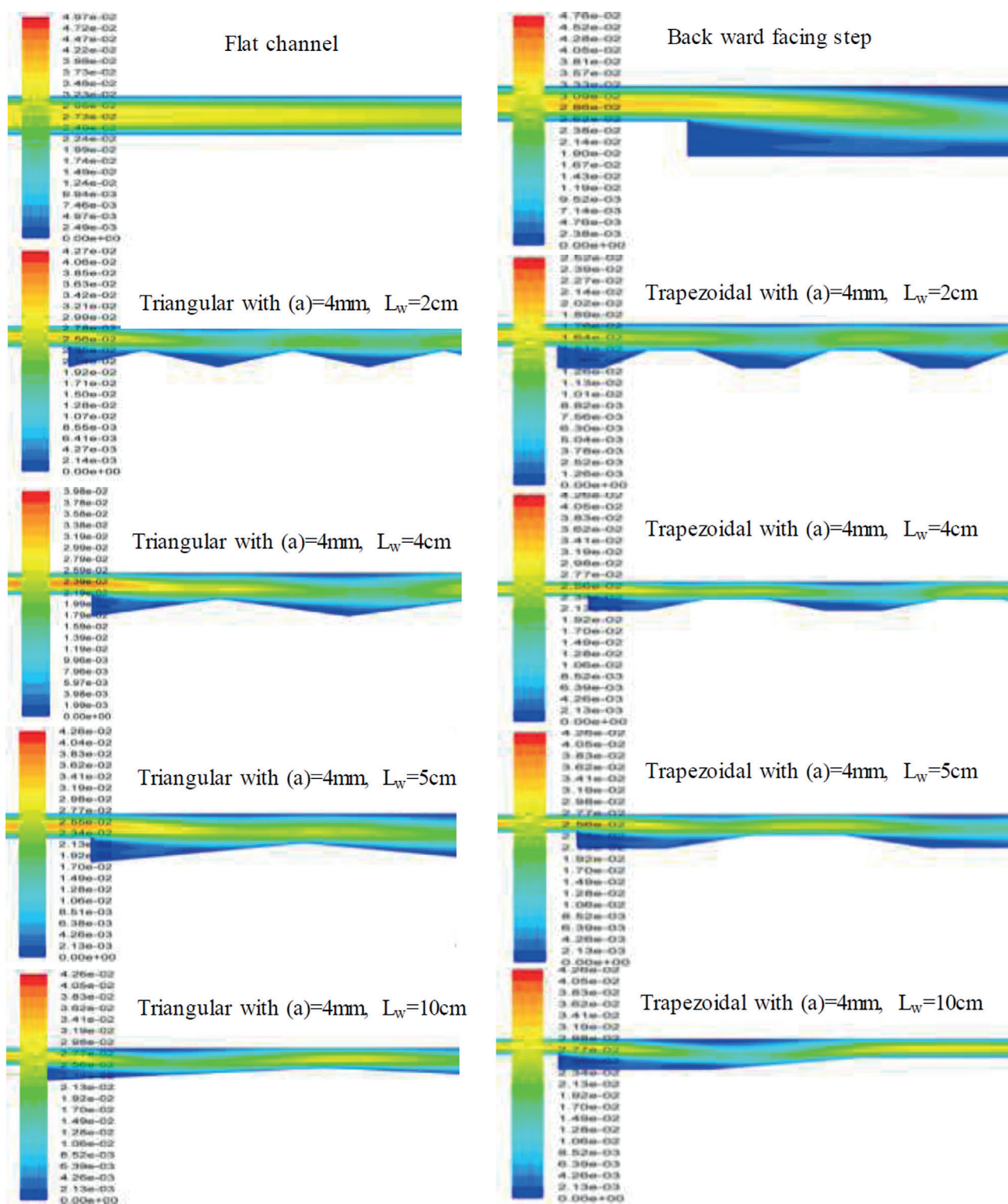


Figure 3. Velocity contours (m/s) for different wavelength (L_w) at constant $Re = 250$, for four different configurations flat channel, backward, Triangular and Trapezoidal facing step channels.

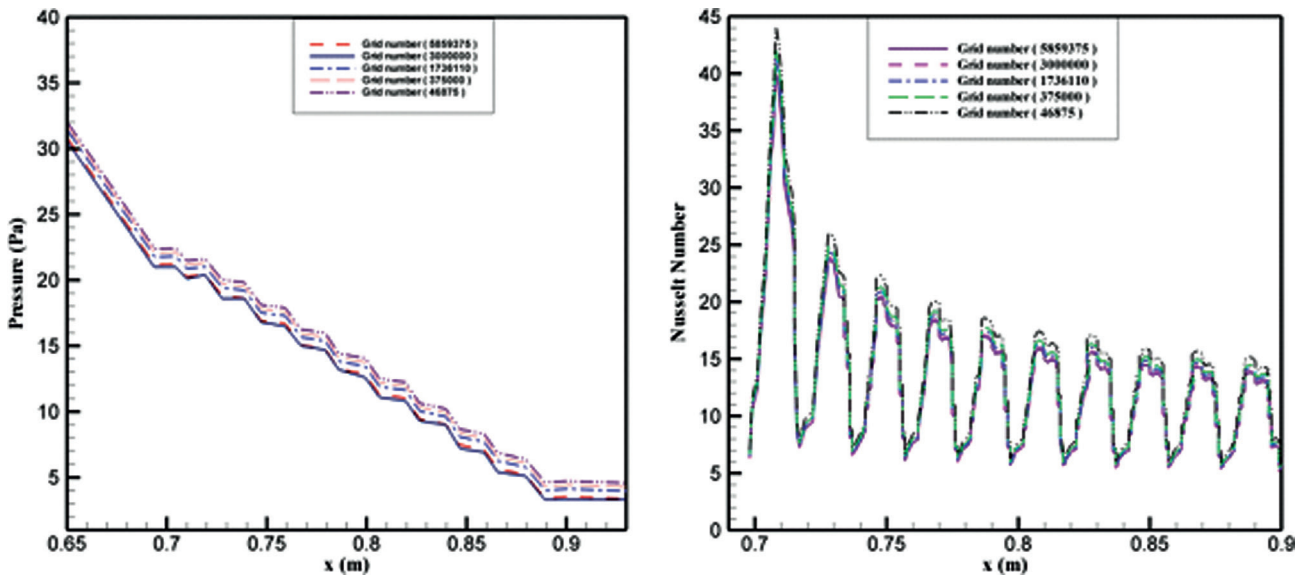


Figure 4. Grid independence test at Reynolds number 100 (pressure distributions(a), Nusselt number(b)).

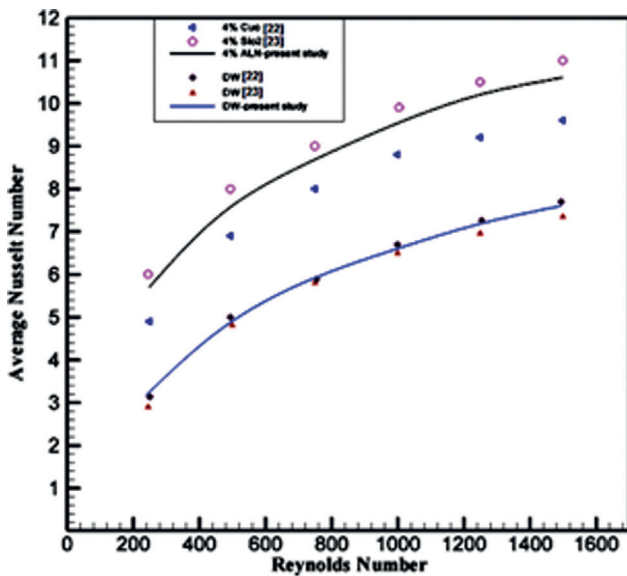


Figure 5. Validation of numerical results with available numerical and experimental data.

Taken into account that; Relative error = $(Nu_{new} - Nu_{previous})/Nu_{new}$

Code Validation

For the purpose of validation, the current study result compared with numerical results of Santra et al. [24], which show a good agreement as shown in Figure 5. In addition, comparison with the results and measured data of Mohammed et al. [25] was carried out for Nusselt number

of 1% of AlN-water nanofluid at $L_w = 20$ mm and $d_p = 30$ nm for the triangular and trapezoidal corrugated channel with amplitude height of 1.5 and 2 mm respectively. The comparison results clearly show a good agreement with an error percentage of 2%.

RESULTS AND DISCUSSION

Although the study was conducted on the four types of channels flat buck step, triangular and trapezoidal, the best results were obtained with triangular and trapezoidal channels. Therefore, the focus in this article will be on these two models and the comparison between them will be on the results achieved through the variation of the wavelength, Reynolds number and nanoparticle concentration.

The effect of triangular and trapezoidal wavelength (L_w) on the Nusselt number, for the wavelength of (2, 4, 5 and 10 cm). is depicted in Figure 6. It is found that the maximum values of Nu were achieved for trapezoidal at a wavelength of 2cm followed by triangular of same wavelength. Since the trapezoidal and triangular channels provide the best fluid mixing due the large size of the re-circulation regions that generated in the diverging sections of the corrugated wall. It is also noticeable that the Nu decreases as the wavelength increase. As the wavelength of corrugated channel increases, the size of re-circulation (secondary) regions will decrease. This means that the intensity of secondary regions in corrugated wall with large wavelength is less than that for the small wavelength. Therefore, the mixing of the fluid in corrugated wall with small wavelength is better than that for large wavelength. Consequently, the wavelength of 2cm will be of main concentration for the rest of this investigation study. In contrast, it can be realise that the maximum

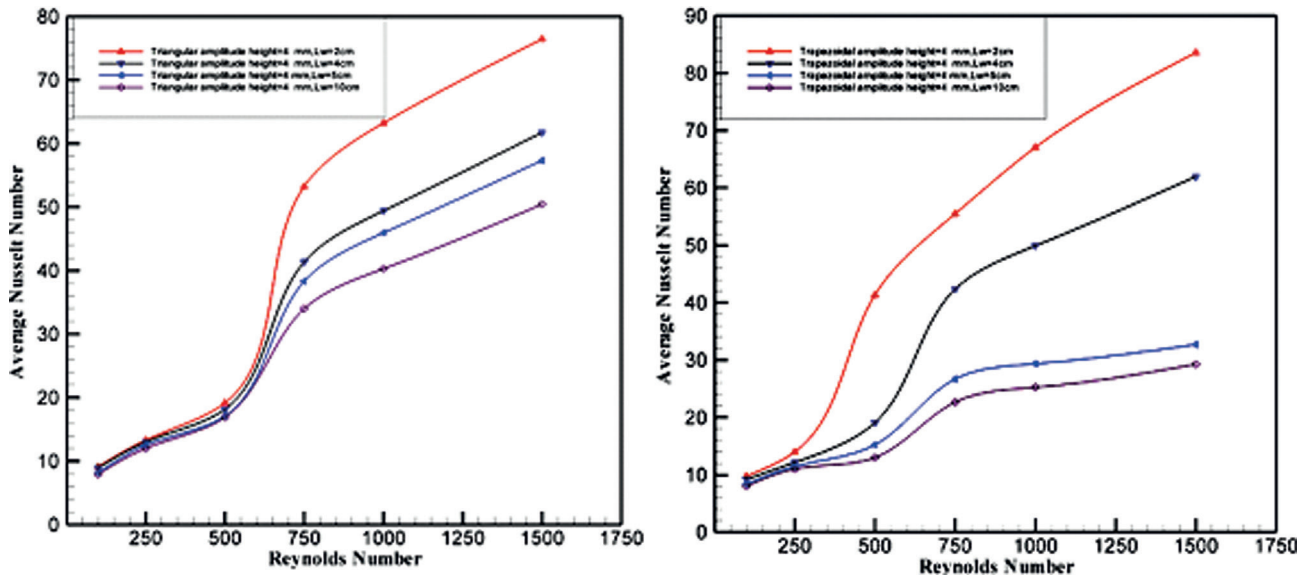


Figure 6: Effect of wavelength on the average Nusselt number (a) triangular corrugated facing step wall (b) trapezoidal corrugated facing step wall at the region of laminar flow.

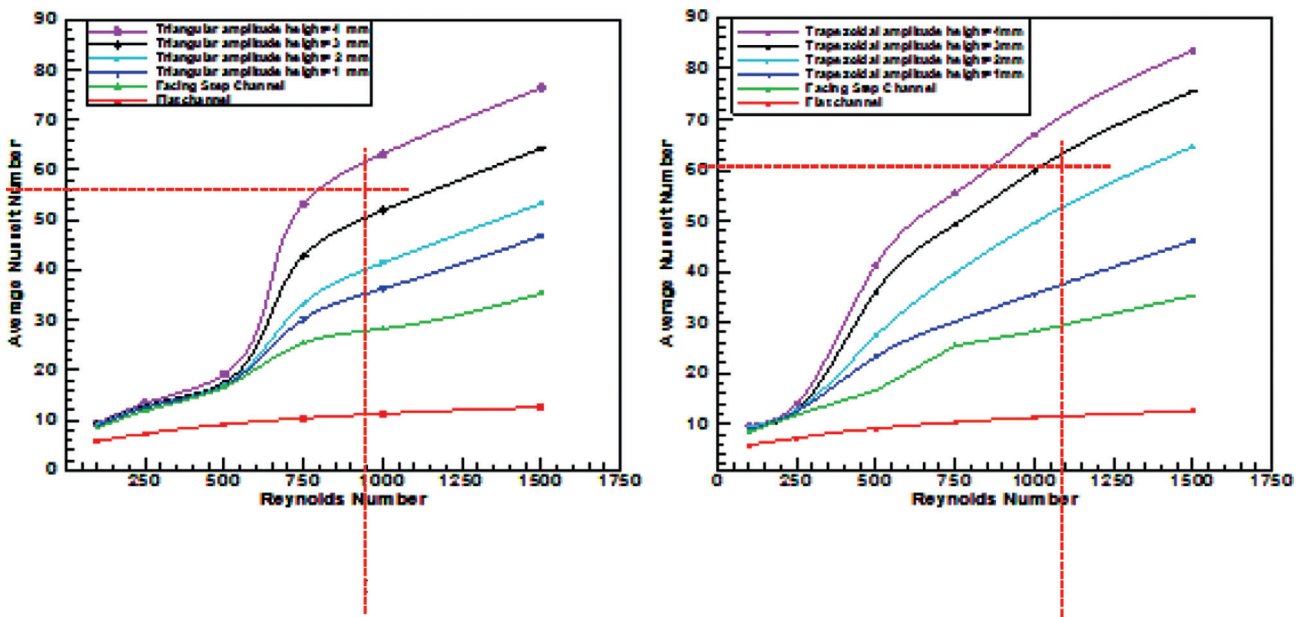


Figure 7. The Influence of channel shape on Nusselt number in the laminar flow region at wavelength of 2 cm (triangular amplitude height (a), trapezoidal amplitude height (b)).

fluid velocity occurs at centreline of channel in converging section (i.e. throat). This is because the corrugated wall has the minimum cross sectional area at this section and since the flow rate of the fluid in channel is constant at any cross section along the channel; therefore, the velocity of the fluid is maximum at the throat of channel. Besides, the velocity gradient at the walls of channel in converging section is the

higher than that at the diverging section. This is consistent with numerical study of Naphon and Kornkumjayrit [26].

In the same way, Figure 7(a) and (b) illustrated the influence of the channel shape on Nusselt number in the laminar region. At Re of 1000, the value of Nusselt number for the trapezoidal wall ($Nu = 67.3$) was obtained in comparison to the triangular wall ($Nu = 63.2$) for the same amplitude

height of 4mm and wavelength L_w of 2cm. It is also confirmed that the Nu increases as the Re increases for the range of 100 to 1500. On line, it can be observed in Figure 7 that higher Nu is achieved for all values of Reynolds number for both the trapezoidal wall and triangular wall with amplitude height of 4mm although the trapezoidal wall has the an advantage over the other shape. This is because the trapezoidal channel provides the best fluid mixing due the

large size of the re-circulation regions that generated in the diverging sections of the corrugated facing step channel.

The effect nanoparticle concentration on the Nusselt number for laminar flow is indicated in Figure 8. Adding an amount of nanopowders to the base fluid is significantly altering the thermophysical properties of the Nanofluid. The higher thermal conductivities of metallic solid powder increase the low thermal conductivity of distilled water when dispersed in. It can be realized that the improvement in the Nusselt number by utilizing AlN-distilled water nanofluid is greater than that by using distilled water. The results obtained here are similar to those brought by Heidary and Kermani [27], which indicate that by increasing the Re number, the average Nu number and the heat transfer from the wall enhance, for various values of nanofluid volume fractions, $\phi = 0, 10, 20\%$.

This improvement can be qualified to the reality that when nanopowders are hanging in the base fluid, the whole thermophysical properties are varied. Nanofluid Prandtl number (Pr) is a function of all these properties of nanofluids. Besides, the growth in the effective thermal conductivity is less than the growth in the effective viscosity. Furthermore, the lower effective density leads to higher effective specific heat capacity. Consequently, nanofluid Prandtl number is higher than Prandtl number for base fluid. For this reason, the Pr for AlN-distilled water nanofluid is greater than that for distilled water and in turn, the heat removal is amplified. Therefore, when Reynolds number (Re_{eff}) number is kept constant, Nusselt number for nanofluid is higher because Nusselt number is a function

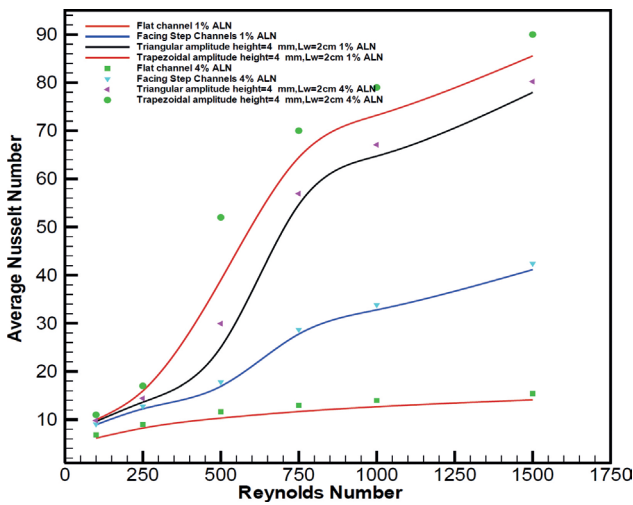


Figure 8. Nanoparticle concentration effect on Nusselt number for laminar flow, 1% and 4% AlN–distilled water.

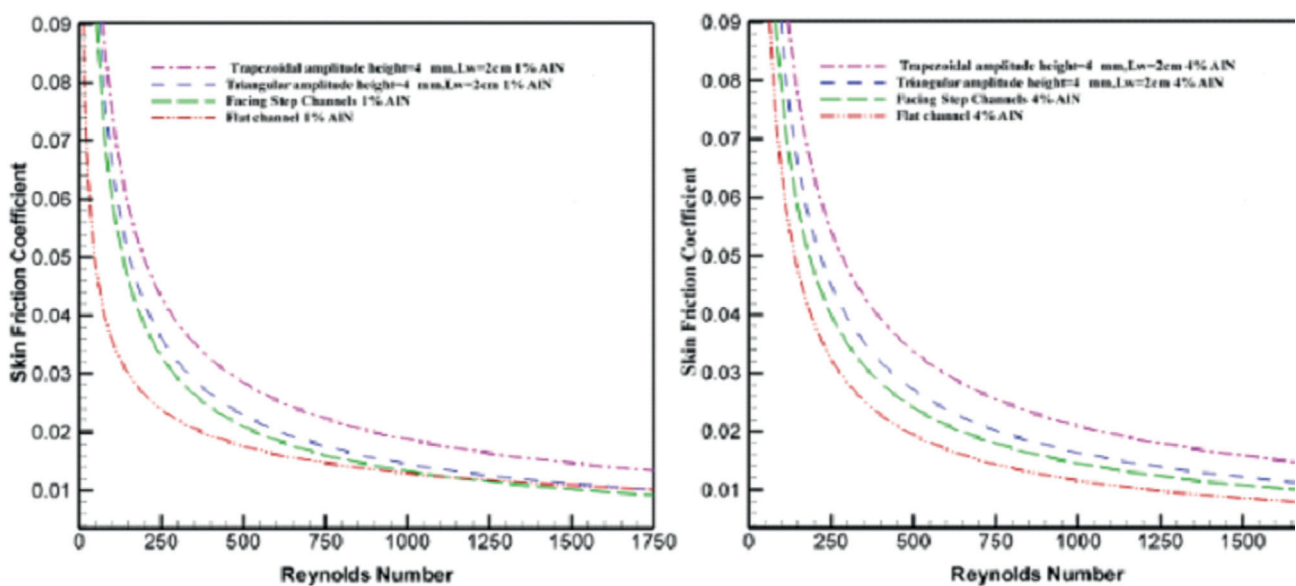


Figure 9. Nanoparticle concentration effect on friction factor for laminar flow (1% AlN – distilled water (a), 4% AlN – distilled water (b)).

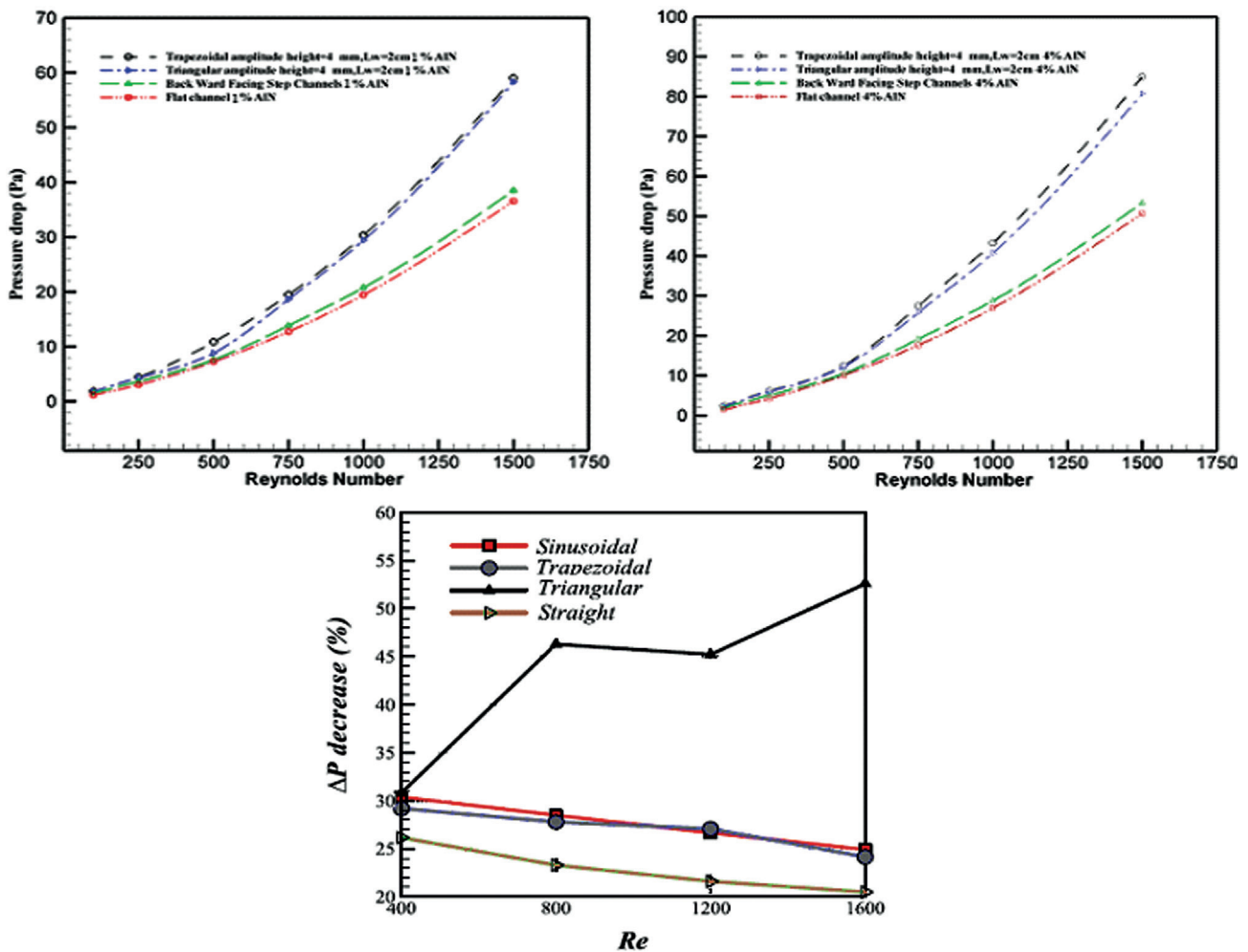


Figure 10. Nanoparticle concentration effect on pressure drop (1% AIN – distilled water (a), 4% AIN – distilled water (b), 3% CuO Nanofluid (c)) modified from [28].

of Pr and Re . Subsequently, nanofluids, having higher Pr , could absorb more heat.

Skin Friction Coefficient

Figure 9 (a) and (b) depicted the effect of adding AlN nanofluid on the skin friction coefficient. This coefficient increases proportionally with the volume fraction ϕ of AlN nanofluid, as it increases from 1% to 4%. This can be impute to the actuality of increasing nanofluid volume fraction will increase viscosity and becomes denser. More viscos fluid restricts the fluid motion in the corrugated wall due to the charming forces between fluid and particles. In the main, the skin friction coefficient decreases with the Re and this decrease is more significant in the laminar flow than the turbulent flow. This decrease in skin friction coefficient is due to the actuality that the hydraulic boundary layer thickness

is became thinner with Re in the laminar flow regime, while there is a slight change in the boundary layer thickness in the turbulent flow regime. In addition, AlN nanofluid display higher friction coefficient than the distilled water due to the reality that AlN nanofluid provides higher velocity than distilled water. So and as mentioned before, the velocity of fluid greatly influences the friction factor in the channel. Lower fluid velocity means higher hydraulic boundary layer thickness and subsequently higher friction factor.

Pressure Drop

Figure 10 (a) and (b) indicated the effect of adding 1% and 4% AlN nanofluid on pressure drop at the region of laminar flow. It is well exposed that the increasing of AlN nanofluid from 1% to 4%, causes the pressure drops to increase significantly from the inlet to the outlet of the duct

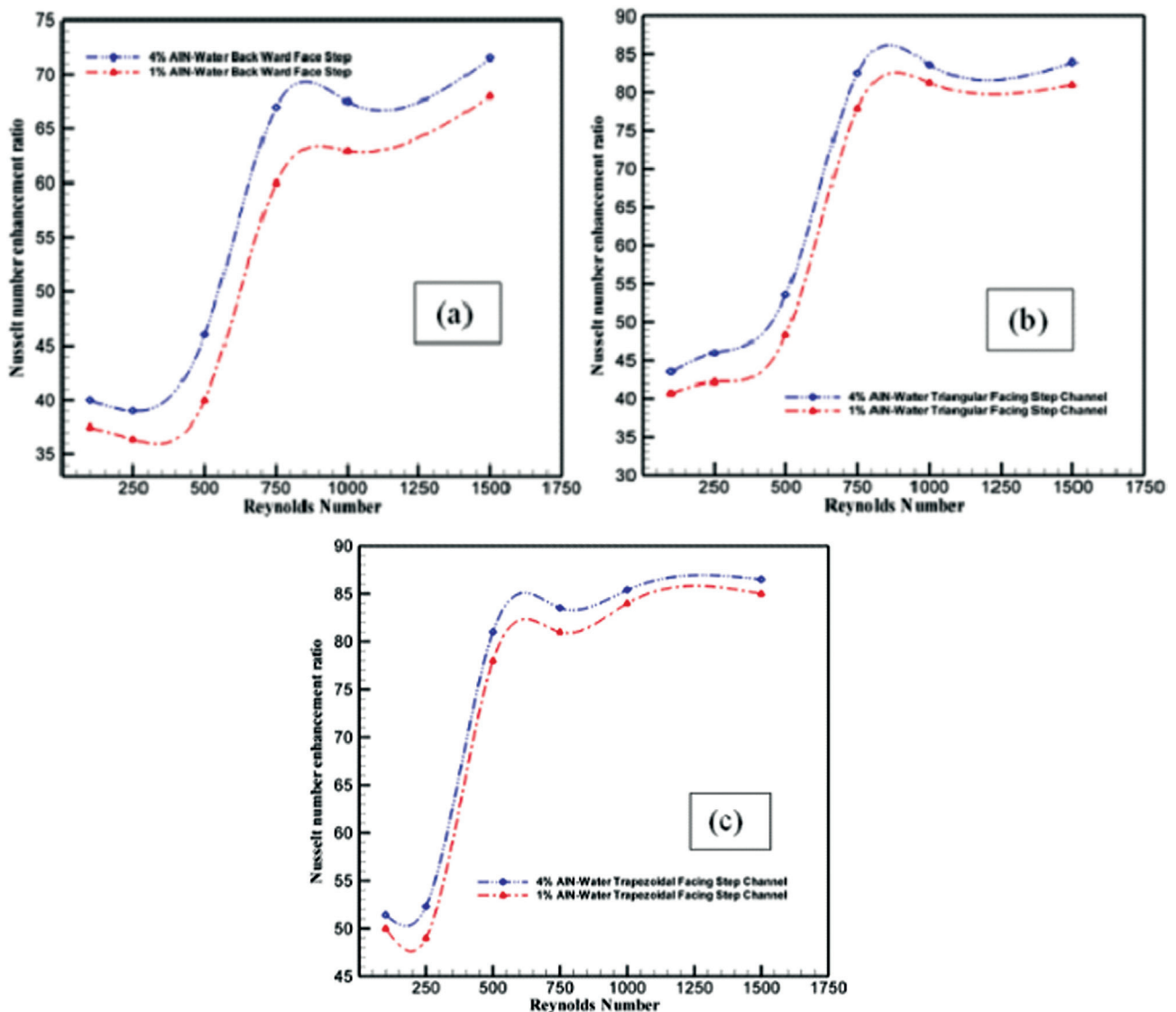


Figure 11. Nusselt number enhancement ratio vs. Reynolds number for different volume fraction of AlN at $a=4$ mm, $L_w=20$ mm and $d_p=25$ nm (backward (a), triangular (b) and trapezoidal facing step channels (c)).

because the suspension of nanoparticles in the base fluid leads to raises in the density and viscosity of the working fluid that's will led to increase pressure drop. Besides, it is found that the highest-pressure drop acquired by the trapezoidal whereas the lowest pressure drop obtained by flat channel for the amplitude height of 4 mm. These results are consistence with the founding of Amin et.al [28]. Their findings from the numerical investigation the force convection flow of non-Newtonian water-CuO Nanofluid, showed that the augmentation of Re and ϕ would result in increasing and decreasing of pressure drops, respectively. The Re intensification from 400 to 1600 results in a significant increase in pressure drop which is more pronounced than

the pressure drop percentage decrease caused by increasing of ϕ as indicated in figure 10(c), adapted from [28].

Nusselt Number Enhancement

The average Nusselt number enhancement ratio for (1 and 4) % AlN - water nanofluid in different channel shapes to the pure water in straight channel is depicted in Figure 11. This enhancement ratio seems to be strongly depends on Reynolds number, amplitude height and channel shapes. The highest enhancement ratio is found in the case of trapezoidal-corrugated facing channel with 4 mm amplitudes height followed by triangular channel for the

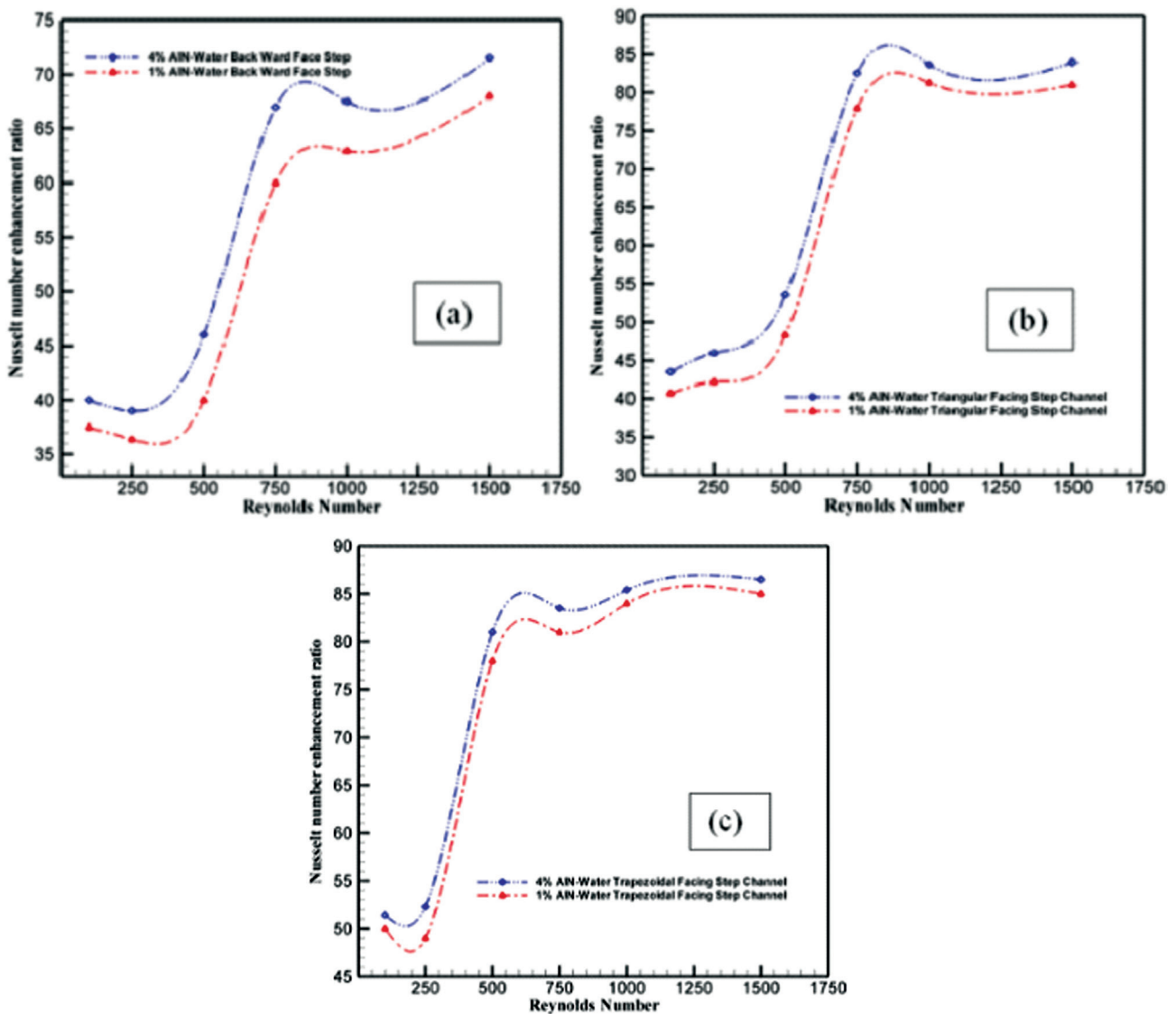


Figure 11. Nusselt number enhancement ratio vs. Reynolds number for different volume fraction of AlN at $a=4$ mm, $L_w=20$ mm and $d_p=25$ nm (backward (a), triangular (b) and trapezoidal facing step channels (c)).

same amplitudes height. It is also observed that as the volume fraction increases from 1% to 4%, the enhancement ratio for backward facing step channel increases from 61 to 71.5 at, while the Nusselt ratio for triangular facing step channel increases from 81 to 84. For trapezoidal channel, it increases from 85 to 87, and these occurs at same $Re = 1500$. Therefore, the using nanofluid with 4% volume fraction in corrugated facing step channels with different shapes display the highest heat transfer enhancement. Finally the average deviation percentage between the numerical and experiment results in literature was around was 3% with the trapezoidal corrugated wall channel.

CONCLUSION

For this study, laminar forced convection heat transfer of AlN–water nanofluid in four type of channels such as flat, back ward, triangle and trapezoidal-corrugated facing step channels have been investigated numerically using finite volume method. The tests were performed for the range of nanoparticle volume fraction is (1%–4 %) and Re of (100–1500). The effects of wavelength (L_w), amplitude height (a), Reynolds number and nanoparticle volume fraction (ϕ) on the skin friction coefficient, pressure drop, and average Nu are presented, analysed and discussed. The results of the numerical investigation offer that the average

Nusselt number (Nu) enhanced with the increasing values of Re , amplitude height of corrugated wall and nanoparticle volume fraction. The skin friction coefficient and pressure drop will also increase. Furthermore, the average Nu decreases as the wavelength of the corrugated wall increases. It is also observed that the addition of AlN-Nano-particles to the distilled water can significantly enhance the heat exchange between the flow and the wall. That is where the use of high nanoparticles volume fractions (4% volume) nanofluid corresponded with the use of four different channel designs resulted in heat transfer augmentation about 30% when compared to that pure water for the trapezoidal channel. Hence, it can be offer to fabricate extra compact heat exchangers with higher mechanical strength, low fabrication costs and higher thermal performance. A comparison of present data with available experimental data in the literature showed the maximum deviation is around 3%.

NOMENCLATURE

a	Amplitude height
AlN	Aluminium Nitride
AR	Aspect ratio
C_f	Darcy friction coefficient
C_p	Specific heat capacity, J/kgK
CFD	Computational Fluid Dynamic
D_h	Hydraulic diameter, m
f	Friction factor
g	Gravitational acceleration, m/s ²
H	Height, m
k	Thermal conductivity, W/mK
K	Boltzmann constant,
L_w	Wavelength
M	Molecular weight, g
Nu	Nusselt number
Pr	Prandtl number
Δp	Pressure difference, pa
Re	Reynolds number
T	Temperature, K
V	Velocity, m/s

Greek symbols

ρ	Density, kg/m ³
ϕ	Volume fraction
μ	Dynamic viscosity, kg/m.s

Subscripts

avr	Average
B	Bulk
bf	Base fluid
eff	Effective
f	Fluid
m	mean
nf	nanofluid

np	nanoparticle
W	Wall
X	Local

AUTHORSHIP CONTRIBUTIONS

Authors equally contributed to this work.

DATA AVAILABILITY STATEMENT

The authors confirm that the data that supports the findings of this study are available within the article. Raw data that support the finding of this study are available from the corresponding author, upon reasonable request.

CONFLICT OF INTEREST

The author declared no potential conflicts of interest with respect to the research, authorship, and/or publication of this article.

ETHICS

There are no ethical issues with the publication of this manuscript.

REFERENCES

- [1] Anoop K, Cox J, Sadr R. Thermal evaluation of nanofluids in heat exchangers. *Int Commun Heat Mass Transf* 2013;49:5–9. [\[CrossRef\]](#)
- [2] Liu XP, Niu JL. Effects of geometrical parameters on the thermohydraulic characteristics of periodic cross-corrugated channels. *Int J Heat Mass Transf* 2015;84:542–549. [\[CrossRef\]](#)
- [3] Alshareef A, Tugolukov EN. Review enhancement of thermal conductivity and heat transfer using carbon nanotube for nanofluids and IO nanofluids. *J Therm Eng* 2021;7:66–90. [\[CrossRef\]](#)
- [4] Geridönmez B, Pekmen, Öztöp Hakan F. Effects of inlet velocity profiles of hybrid nanofluid flow on mixed convection through a backward facing step channel under partial magnetic field. *Chem Phys* 2021;540:111010. [\[CrossRef\]](#)
- [5] Abu-Mulaweh HI. Investigations on the effect of backward-facing and forward-facing steps on turbulent mixed-convection flow over a flat plate. *Exper Heat Transf* 2009;22:117–127. [\[CrossRef\]](#)
- [6] Barkley D, Gabriela M, Gomes M, Ronald D. Three-dimensional instability in flow over a backward-facing step. *J Fluid Mech* 2002;473:167–190. [\[CrossRef\]](#)
- [7] Armaly BF, Li A, Nie J. Measurements in three-dimensional laminar separated flow. *Int J Heat Mass Transf* 2003;46:3573–3582. [\[CrossRef\]](#)

- [8] Sherry M, Jacono DL, Sheridan J. An experimental investigation of the recirculation zone formed downstream of a forward facing step. *J Wind Eng Ind Aerodynamics* 2010;98:888–894. [\[CrossRef\]](#)
- [9] Sivakumar A, Sathiyamoorthi R, Alagumurthi N, Jayaseelan V, Sudhakar K. Thermal performance of U-shaped serpentine microchannel heat sink using various metal oxide nanofluids. *Heat Transf* 2021;50:3094–3118. [\[CrossRef\]](#)
- [10] Mohammed MK, Abdolbaqi MK, Ibrahim TK, Bin Mamat R, Awad OI. Experimental and numerical investigation of heat transfer enhancement using al2o3-ethylene Glycol/Water nanofluids in straight channel. *MATEC Web of Conferences* 2018;225:01019. [\[CrossRef\]](#)
- [11] Abu-Nada E. Application of nanofluids for heat transfer enhancement of separated flows encountered in a backward facing step. *Int J Heat Fluid Flow* 2008;29:242–249. [\[CrossRef\]](#)
- [12] Kherbeet AS, Mohammed H, Salman B. The effect of nanofluids flow on mixed convection heat transfer over microscale backward-facing step. *Int J Heat Mass Transf* 2012;55:5870–5881. [\[CrossRef\]](#)
- [13] Bayareh M, Nourbakhsh A. Numerical simulation and analysis of heat transfer for different geometries of corrugated tubes in a double pipe heat exchanger. *J Therm Eng* 2019;5:293–301. [\[CrossRef\]](#)
- [14] Al-Aswadi AA, Mohammed HA, Shuaib NH, Campo A. Laminar forced convection flow over a backward facing step using nanofluids. *Int J Commun Heat Mass Transf* 2010;37:950–957. [\[CrossRef\]](#)
- [15] Ghachem K, Aich W, Kolsi L. Computational analysis of hybrid nanofluid enhanced heat transfer in cross flow micro heat exchanger with rectangular wavy channels. *Case Stud Therm Eng* 2021;24:100822. [\[CrossRef\]](#)
- [16] Kilic M, Muhammad AH. Numerical investigation of combined effect of nanofluids and multiple impinging jets on heat transfer. *Therm Sci* 2019;23:3165–3173. [\[CrossRef\]](#)
- [17] Plant RD, Saghir MZ. Numerical and experimental investigation of high concentration aqueous alumina nanofluids in a two and three channel heat exchanger. *Int J Thermofluids* 2021;9:100055. [\[CrossRef\]](#)
- [18] Mohammed KA, Abu Talib AR, Abdul Aziz N, Ahmed KA. Three dimensional numerical investigations on the heat transfer enhancement in a triangular facing step channels using nanofluid. *IOP Conf Series Mater Sci Eng* 2016;152:012057. [\[CrossRef\]](#)
- [19] Ghasemi B, Aminossadati S. Natural convection heat transfer in an inclined enclosure filled with a water-CuO nanofluid. *Num Heat Transf Part A Appl* 2009;55:807–823. [\[CrossRef\]](#)
- [20] Vajjha RS, Das DK. Experimental determination of thermal conductivity of three nanofluids and development of new correlations. *Int J Heat Mass Transf* 2009;52:4675–4682. [\[CrossRef\]](#)
- [21] Corcione M. Heat transfer features of buoyancy-driven nanofluids inside rectangular enclosures differentially heated at the sidewalls. *Int J Therm Sci* 2010;49:1536–1546. [\[CrossRef\]](#)
- [22] Eiamsa-Ard S, Promvong P. Thermal characteristics of turbulent rib-grooved channel flows. *Int Commun Heat Mass Transf* 2009;36:705–711. [\[CrossRef\]](#)
- [23] Anderson JD. *Computational Fluid Dynamic: The Basics with Applications*. New York:McGraw-Hill; 1995.
- [24] Santra AK, Sen S, Chakraborty N. Study of heat transfer due to laminar flow of copper-water nanofluid through two isothermally heated parallel plates. *Int J Therm Sci* 2009;48:391–400. [\[CrossRef\]](#)
- [25] Mohammed A, Yusoff M, Ng K, Shuaib N. Numerical and experimental investigations on the heat transfer enhancement in corrugated channels using SiO₂-water nanofluid. *Case Stud Therm Eng* 2015;6:77–92. [\[CrossRef\]](#)
- [26] Naphon P, Kornkumjayrit K. Numerical analysis on the fluid flow and heat transfer in the channel with V-shaped wavy lower plate. *Int Commun Heat Mass Transf* 2008;35:839–843. [\[CrossRef\]](#)
- [27] Heidary H, Kermani M. Effect of nano-particles on forced convection in sinusoidal-wall channel. *Int Commun Heat Mass Transf* 2010;37:1520–1527. [\[CrossRef\]](#)
- [28] Shahsavar A, Alimohammadi S, Baniasad Askari I, Ali H. Numerical investigation of the effect of corrugation profile on the hydrothermal characteristics and entropy generation behavior of laminar forced convection of non-Newtonian water/CMC-CuO nanofluid flow inside a wavy channel. *Int Commun Heat Mass Transf* 2021;121:105117. [\[CrossRef\]](#)